Measurement of the capillary interaction force between Janus colloidal particles trapped at a flat air/water interface†

Virginia Carrasco-Fadanelli and Rolando Castillo (iD) *

The capillary interaction force between spherical Janus particles trapped at the air–water interface is measured using a time-sharing optical tweezer (bond number $\ll$ 1). One face of the particles is hydrophilic, and the other one, hydrophobic. Measured force goes from almost pure quadrupolar to almost pure hexapolar interaction due to the three-phase contact line corrugation. Measured force curves are modeled as a sum of power laws, $Ar^{-\alpha} + Br^{-\beta} + Cr^{-\gamma}$, obtained from an expansion in capillary multipoles. The mean values for the exponents of particle pairs of 3 μm are $\langle\alpha\rangle = 5.05 \pm 0.12$, $\langle\beta\rangle = 7.02 \pm 0.03$, and $\langle\gamma\rangle = 5.96 \pm 0.03$. For particles pairs of 5 μm, we find $\langle\alpha\rangle = 5.02 \pm 0.04$, $\langle\beta\rangle = 6.94 \pm 0.06$, and $\langle\gamma\rangle = 5.80 \pm 0.05$. In both cases, $A < 0$, $B < 0$, and $C > 0$.

In his Nobel Prize address, P. G. de Gennes[1] raised the concept of Janus Particles (JPs) based on the work of Casagrande and Veyssié.[2] A few years before he also suggested that the solid–liquid–vapor contact line must have an irregular shape, to explain the contact angle hysteresis in partial wetting. This line is pinned on nanoscopic sites due to roughness or chemical heterogeneities on the solid surface.[3] The anchorage of the triple line on defects of the solid surface and its dynamics have significant consequences on the behavior of colloidal particles trapped at interfaces.

Free energy traps standard colloids irreversibly at interfaces. When gravity is negligible (Bond number = capillarity length/particle radius $\ll$ 1), the interface where colloidal particles are trapped should not be deformed. If the particle straddling on the surface is at equilibrium, the contact angle entirely determines its flotation level, as required by Young's law. Nevertheless, the interface close around the particles is still deformed due to the irregular shape of the contact line. Then, particles trapped on a planar interface can strongly interact to lower surface energy, even when they are not charged.[4]

Janus Particles (JPs) are colloids composed of two hemispherical surfaces that differ in their physical and chemical

properties, often contrary in nature. In our case, one of them is hydrophobic, and the other is hydrophilic. Although it is commonly accepted that at equilibrium, they are adsorbed at the A/W interface with their symmetry axis perpendicular to the interface, there is evidence that it could be tilted in a none-quilibrium state.[5] This leads to an inter-particle interaction with a complex angular contribution, as well as a contribution inversely proportional to the third power of the inter-particle distance.[6] In amphiphilic JPs, it is also necessary to consider the Janus balance, which determines their flotation level that is not necessarily the boundary line between the hydrophobic and hydrophilic areas because this configuration does not necessarily correspond to the maximum absorption energy.[7] Besides, this boundary line is not necessarily sharp and smooth. It is corrugated due intrinsically to the synthetic methods of preparation of JPs.[5,8,9]

Park *et al.*,[5] measured the attractive interaction between JPs straddling at the decane/W interface using particle trajectory analysis and estimating the drag force of particles. Despite this is not a very accurate method to measure this interaction, their data is consistent with a capillary interaction of the form $F \sim r^{-5}$. Nevertheless, their results present significant fluctuation in the exponent, and in the magnitude of the interaction force that varied with the measured particle pairs. They did not observe electrostatic interaction due to dipolar interaction. In this communication, we present precise measurements addressed to determine the capillary interaction force between JPs trapped at the air–water (A/W) interface due to the three-phase contact line corrugation. We will show that quadrupolar interaction used in standard spherical and homogeneous colloids is not enough to explain the capillary interaction between JPs. With our results, we understand some of the curious behavior of JPs trapped at interfaces.

It is necessary to mention that JPs inevitably inherit some features observed in standard colloids straddling at interfaces. Although they are not directly studied in these colloids. Namely, (a) No noticeable deformation of the interface has been observed around the interface in the range of a few micrometers around the particle position.[10] However, it has been found a relation

Instituto de Física, Universidad Nacional Autónoma de México, P.O. Box 20-364, México City, 01000, Mexico. E-mail: rolandoc@fisica.unam.mx

between particle immersion and diffusion based on thermally activated fluctuations of the interface at the triple line. They are coupled to the particle drag, driving the system out of mechanical equilibrium and producing extra random forces on the particle. (b) Details of the approaching process to an interface, the moment it breaches, and the slow logarithmic time relaxation that follows have been observed.[11] The observed dynamics agree with a model describing activated hopping of the contact line over nanoscale surface heterogeneities, resembling the aging dynamics in glassy systems. (c) Normal interactions of colloids with interfaces can also modify the lateral interactions, which depend on the salt concentration of the fluids associated with the interface.[12] Therefore, JPs trapped at interfaces present new challenges for understanding their behavior, which is different from that observed when they are spread in bulk. For these reasons, it is relevant to understand the interaction between these particles that have attracted much attention in recent years. Their novel properties can exhibit great potential in unique applications as interfacial stabilizers, Pickering emulsions, biomedicine, electrochemical applications, etc.[13–16]

Stamou et al.[4] theoretically derived a lateral attraction between uncharged microspheres with homogeneous surfaces trapped at the A/W interface, whose origin is the irregular shape of the contact line, and its associated distortion of the water surface. Capillary interaction occurs between particles because they are committed to minimizing the interfacial area to lower Free Energy. They calculated the shape of the interface around a colloidal particle, $h(r,\varphi)$, as a multipolar expansion given by:

$$h(r,\varphi) = \sum_{m=0}^{\infty} H_m \cos\left(2\left(\varphi - \varphi_{m,0}\right)\right)\left(\frac{r}{r_c}\right)^m, \qquad (1)$$

where r and φ are the cylindrical coordinates, $\varphi_{m,0}$ is a reference angle, H_m is a coefficient that gives the height of the meniscus at contact, r_c. Evaluating the boundary conditions on the particle that results to be the contact line, they found for homogeneous particles that the most important term in the series is when $m = 2$. For two interacting particles, the authors found the most relevant term of the interaction potential, which has been confirmed by others,[17] as:

$$V(r) = -12\pi\gamma H_2^A H_2^B \cos[2(\varphi_{A0} + \varphi_{B0})](r_c/r)^4, \qquad (2)$$

where γ is the liquid surface tension, φ_{i0} are orientation angles of the interacting particles, A and B, relative to a line joining their centers. Therefore, when interface deformations of neighboring particles overlap, particles rotate and approach each other. So, they assemble to minimize the interfacial area excess. The interaction force between uncharged colloidal particles trapped at the A/W interface depends on distance as a r^{-5}. This result was confirmed recently by us employing precise measurements.[18]

Our JPs are nonmetallic and prepared using the protection-deprotection method reported in ref. 8 and 9. Silica particles of 3 μm and 5 μm are adsorbed on molten drops of a paraffine wax-in-water emulsion with a surfactant (didodecyldimethyl-ammonium bromide) to control their dipping level. After cooling,

the exposed surface of the particles at the created colloidosomes is chemically modified with a vapor of dichlorodimethylsilane. The resulting JPs are dispersed in chloroform and deposited with a syringe on an A/W (Nanopure-UV, resistivity > 18.3 MΩ cm) interface in a Langmuir trough, at $T = 23$ °C. Particles are trapped with a time-shared optical tweezer in the same way as previously done to measure the interaction between standard spherical colloids (Fig. S1a, ESI†).[18] We use the Boltzmann distribution method[18,19] for calibrating the tweezers. Particle positions are acquired with a video camera and standard software for tracking.[20] The displacements of each JP, δx_i, from their equilibrium position at the center of the optical trap, are due to the interaction between them. Fig. S2b ESI† shows the model considered in our experiments.[18] Springs constrain particles because the optical tweezers behave as harmonic potentials, such that the force exerted on the particles is given by $F_i = k_i\delta x_i$, where k_i is the stiffness constant of the optical trap, and $i = 1, 2$. The interaction force between a pair of JPs is obtained measuring the average displacement from the center of the optical trap of each particle as they approach. However, when the particles are at a certain distance, if the force gradient is larger than the effective constant, the system becomes unstable, and particles jump into contact. In our case, the stiffness constant can be controlled by modulating the laser power in the trap (see Fig. S2c, ESI†) to minimize this effect.[18]

Fig. 1 presents examples of the interaction forces between pairs of JPs of 3 μm, selected at random when they are adsorbed at the A/W interface. Different colors correspond to measurements
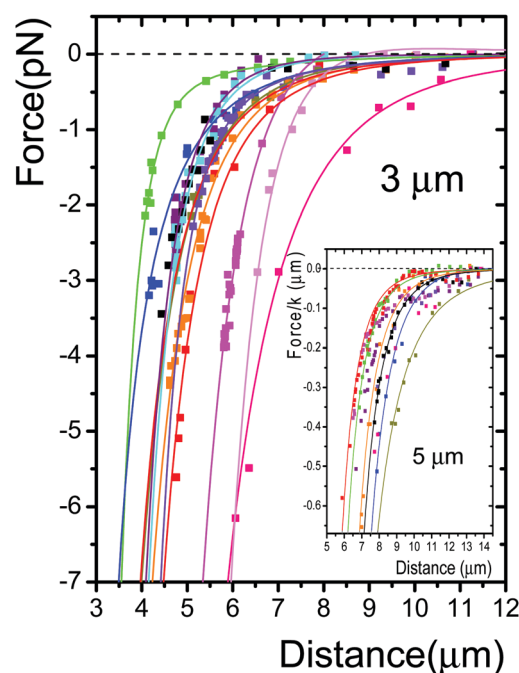

Fig. 1 The capillary interaction force between Janus colloidal particles adsorbed at the A/W interface of a diameter of 3 μm. Inset b: F/k for particles of a diameter of 5 μm. Color denotes different experiments. Curves are fittings of eqn (5) to data. This data is presented in a log–log plot in Fig. S3 ESI.†
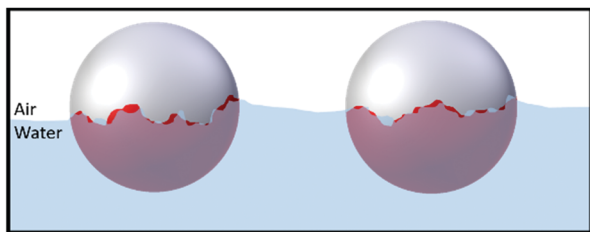
Fig. 2   The three-phase contact line in JPs (red hydrophilic face, light gray hydrophobic face, and light blue W) that do not necessarily follow the irregular hydrophilic–hydrophobic boundary. The corrugation of the contact line can be different for each JP particle in an interacting pair.

on different pairs of JPs. The interaction between couples of particles is attractive, in the range of a few pNs. The force curves are different for each pair, and just some of the measurements can be fitted to a r^{-5} power-law. Other measurements do not follow this power law (not shown). To focus our interest on the exponents of the interaction, the inset in Fig. 1 presents measurements of F/k for Janus particle pairs of 5 μm, also selected at random.

To explain the dispersion of data, we need to consider that the three-phase contact line might not follow the hydrophobic–hydrophilic boundary line, which was generated during the synthesis of the JPs. The interface shape around particles in a wax/W liquid interface must follow eqn (1), and at the boundary (r_c), the most relevant term must be when $m = 2$. Force measurements between particles at interfaces support this assumption.[18,21] Then, the boundary line is also corrugated. On the A/W interface, we can consider that depending on how W is pinned on the nanoscopic surface defects of the JPs, contact lines might be more corrugated in some JPs than in others (Fig. 2). This increase in corrugation, inevitably, would be reflected in the total interaction force between particle pairs. Therefore, the contact line, as given by the boundary condition in eqn (1), must include not only the term when $m = 2$. Taking into account the next term in $h(r,\varphi)$, for each particle of the interacting pair, we obtain:

$$h(r, \varphi) = H_2 \cos(2(\varphi - \varphi_2))\frac{r_c^2}{r^2} + H_3 \cos(3(\varphi - \varphi_3))\frac{r_c^3}{r^3}. \quad (3)$$

The interaction potential between JP pairs, calculated in the same way as in ref. 4 gives:

$$V = -\frac{12\gamma\pi H_2^A H_2^B r_c^4 \cos(2(\varphi_A - \varphi_B))}{r^4}$$

$$- \frac{60\gamma\pi H_3^A H_3^B r_c^6 \cos(3(\varphi_A - \varphi_B))}{r^6}$$

$$+ \frac{24\gamma\pi r_c^5 \left[H_3^A H_2^B \cos(3\varphi_A - 2\varphi_B) + H_2^A H_3^B \cos(2\varphi_A - 3\varphi_B) \right]}{r^5}. \quad (4)$$

The first two terms in eqn (4) correspond to attractive interactions (quadrupolar and hexapolar), and the last one corresponds to a repulsive cross-interaction. Fig. 3 shows examples of the interaction calculated with eqn (4), varying the H_m values, when the quadrupolar and hexapolar terms are of the same order
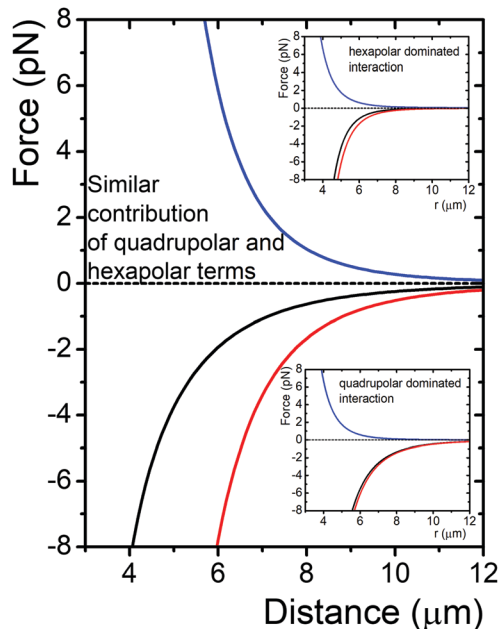

Fig. 3   Calculated net capillary interaction (black) for JP of 3 μm, when the quadrupolar and hexapolar contributions are of the same order. Blue and red lines are the repulsive and the sum of attractive terms, respectively. Insets present the interactions when the quadrupolar or hexapolar terms dominate.

($H_2 \sim H_3$). The resultant capillary force is the black line; blue and red lines are the repulsive and the sum of attractive terms, respectively. When the contribution of the quadrupolar is smaller than the hexapolar one ($H_2 < H_3$, top inset Fig. 3), the net force becomes completely attractive, and the hexapolar term dominates the interaction. The opposite occurs when the hexapolar term is small ($H_2 > H_3$, bottom inset Fig. 3). Then, as the interface deformations of neighboring particles overlap, particles rotate to reach a specific orientation value, and they approach each other urged by $-\nabla V$, given by:

$$F = \frac{A}{r^\alpha} + \frac{B}{r^\beta} + \frac{C}{r^\gamma}, \quad (5)$$

eqn (5) is used to fit the experimental data (curves in Fig. 1). The mean values for the exponents of particle pairs of 3 μm are $\langle\alpha\rangle = 5.05 \pm 0.12$, $\langle\beta\rangle = 7.02 \pm 0.03$, and $\langle\gamma\rangle = 5.96 \pm 0.03$. For particles pairs of 5 μm, we find $\langle\alpha\rangle = 5.02 \pm 0.04$, $\langle\beta\rangle = 6.94 \pm 0.06$, and $\langle\gamma\rangle = 5.80 \pm 0.05$. In both cases, $A < 0$, $B < 0$, and $C > 0$, in agreement with the $-\nabla V$.

Force measurements show high sensitivity to the particular details of the contact line corrugation of the particles involved in the measure. Depending on the measured particle pair, capillary interaction can go from quadrupolar to hexapolar. From all measurements, approximately 40% are dominated by the quadrupolar interaction, $F \sim A/r^5$. Here, probably the contact line and the hydrophilic–hydrophobic boundary coincide. On the contrary, 20% of the measurements are dominated by the hexapolar interaction, $F \sim A/r^7$. Here, the contact line necessarily is more corrugated than in the former case. So, this line does not coincide with the original boundary determined by the synthesis
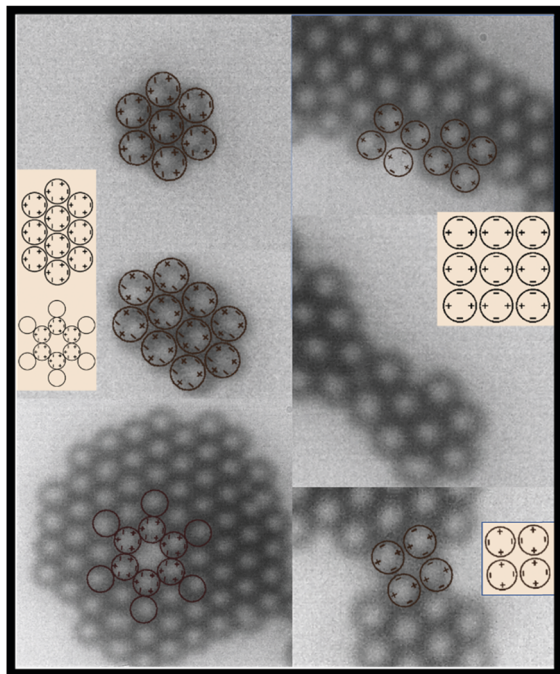
Fig. 4 Clusters observed during our force measurements where hexapolar (hexagonal arrays) or quadrupolar interaction (square arrays) dominate. In some images, we superimposed the clusters shown in the colored insets predicted by Danov et al.[17] for the mentioned interactions. Signs represent the maxima and minima of the contact line undulations.

with $m = 2$ (see Fig. 2). The average value for H_2 can be estimated; pure quadrupolar $H_2 \sim 26$ nm, and pure hexapolar $H_3 \sim 70$ nm. For the remaining 40% of the measurements, the quadrupolar and hexapolar interactions are approximate of the same size. Clusters showing when some of these interactions dominate are not commonly observed. We were able to capture some JP clusters with these features during our measurements, see Fig. 4. They do not represent any averaging. We mainly selected clusters where hexapolar interaction is significant, like those predicted by Danov et al,[17] which are unusually observed; square lattice clusters are underrepresented here. Note one cluster with hexagonal order but without a central particle. Ordering in monolayers of JP particles at the A/W interface can be found in ref. 22.

The range of interactions for hexapolar and quadrupolar interactions is different. Hexapolar interactions become relevant at very short scales that are not accessible to our experiments, due to the jump into contact, even at the high k values that we used. At the separation distances where we made our measurements ($r > 1$ µm), the quadrupolar and hexapolar contributions for $H_2 \approx H_3$ are of the same order of magnitude, as given by eqn (4). When $H_2 < H_3$, the quadrupolar contribution is smaller than the hexapolar contribution. On the contrary, when $H_2 > H_3$, the quadrupolar contribution is more significant than the hexapolar contribution. Quadrupolar or hexapolar preponderance depends not only on the separation distance of the particles but also on the H_2 and H_3 values. At distances shorter than 1 µm, the situation could be different. Here, van der Waals's interaction starts to play.

As in ref. 5, we neither observe electrostatic interaction due to electric dipolar interaction, nor interactions of the form r^{-3} (capillary dipolar interaction)[6] attributed to tilted nonequilibrium orientations. However, optical trapping and the handling of the particles to bring them together could give the necessary energy to reach the equilibrium configuration. However, the hexagonal order found in monolayers of JPs at the air/W interface can be explained now by the contribution of the hexapolar interaction and not a capillary dipolar interaction, as assumed in ref. 22.

In summary, the origin of the interaction between uncharged colloidal particles straddling at the A/W interface is due to the corrugated shape of the contact line, in agreement to the model of Stamou et al.[4] Although, in JPs, it is necessary to include more terms in the multipolar expansion that leads to a force given by a sum of three independent power laws, as given by eqn (4).

Conflicts of interest

There are no conflicts to declare.

Acknowledgements

References

1 P. G. de Gennes, Soft Matter Nobel Lecture, 1991.
2 C. Casagrande, P. Fabre, E. Rraphaël and M. Veyssié, *Europhys. Lett.*, 1989, **9**, 251.
3 P. G. de Gennes, *Rev. Mod. Phys.*, 1985, **57**, 827.
4 D. Stamou, C. Duschl and D. Johannsmann, *Phys. Rev. E: Stat. Phys., Plasmas, Fluids, Relat. Interdiscip. Top.*, 2000, **62**, 5263.
5 B. J. Park, T. Brugarolas and D. Lee, *Soft Matter*, 2011, **7**, 6413.
6 H. Rezvantalab and S. Shojaei-Zadeh, *Soft Matter*, 2013, **9**, 3640.
7 S. Jiang and S. Granick, *J. Chem. Phys.*, 2007, **127**, 161102.
8 S. Jiang, M. J. Schultz, Q. Chen, J. S. Moore and S. Granick, *Langmuir*, 2008, **24**, 10073.
9 L. C. Mugica, B. Rodríguez-Molina, S. Ramos and A. Kozina, *Colloids Surf., A*, 2016, **500**, 79.
10 G. Boniello, C. Blanc, D. Fedorenko, M. Medfai, N. B. Mbarek, M. In, M. Gross, A. Stocco and M. Nobili, *Nat. Mater.*, 2015, **14**, 908.
11 D. M. Kaz, R. McGorty, M. Man., M. P. Brenner and V. N. Manoharan, *Nat. Mater.*, 2012, **11**, 138.
12 A. Wang, J. W. Zwanikken, D. M. Kaz, R. McGorty, A. M. Goldfain, W. B. Rogers and V. N. Manoharan, *Phys. Rev. E*, 2019, **100**, 042605.
13 A. Walther and A. H. E. Müller, *Chem. Rev.*, 2013, **113**, 5194.
14 B. Haney, D. Chen, L. H. Cai, D. Weitz and S. Ramakrishnan, *Langmuir*, 2019, **35**, 4693.

15 P. Yanez-Sedeno, S. Campuzano and J. M. Pingarron, *Appl. Mater. Today*, 2017, **9**, 276–288.

16 H. Su, C. A. Hurd Price, L. Jing, Q. Tian, J. Liu and K. Qian, *Mater. Today. Bio.*, 2019, **4**, 100033.

17 K. D. Danov, P. A. Kralchevsky, B. N. Naydenovand and G. Brenn, *J. Colloid Interface Sci.*, 2005, **287**, 121.

18 V. Carrasco-Fadanelli and R. Castillo, *Soft Matter*, 2019, **15**, 5815.

19 M. Sarshar, W. T. Wong and B. Anvari, *J. Biomed. Opt.*, 2014, **19**, 115001.

20 S. V. Franklin and M. D. Shattuck, *Handbook of Granular Materials*, Taylor & Francis, Boca Raton, ch. 2, 2016.

21 B. J. Park and E. M. Furst, *Soft Matter*, 2011, **7**, 7676.

22 A. Kozina, S. Ramos, P. Díaz-Leyva and R. Castillo, *J. Phys. Chem. C*, 2016, **120**, 16879.